

## Recent results from LHCb on semileptonic decays of b hadrons

---

**Concezio Bozzi**<sup>\*†</sup>

*CERN and INFN Sezione di Ferrara*

*E-mail:* [bozzi@fe.infn.it](mailto:bozzi@fe.infn.it)

Recent results on semileptonic decays of  $b$  hadrons at LHCb are presented, with particular emphasis on decays involving  $\tau$  leptons in the final state. A new measurement of  $\mathcal{R}(D^{*-}) \equiv \mathcal{B}(B^0 \rightarrow D^{*-} \tau^+ \nu_\tau) / \mathcal{B}(B^0 \rightarrow D^{*-} \mu^+ \nu_\mu)$  is reported, by using for the first time the  $\tau$  lepton decays with three charged pions in the final state. A value of  $\mathcal{R}(D^{*-}) = 0.285 \pm 0.019 \pm 0.025 \pm 0.013$  is obtained, where the first uncertainty is statistical, the second systematic and the third uncertainty is due to the limited knowledge of external branching fractions. This measurement is in agreement with the Standard Model prediction and with previous results.

*The European Physical Society Conference on High Energy Physics*

*5-12 July, 2017*

*Venice*

---

<sup>\*</sup>Speaker.

<sup>†</sup>on behalf of the LHCb Collaboration

## 1. Semileptonic decays of $b$ hadrons and tests of Lepton Flavour Universality

Semileptonic decays of  $b$  hadrons give access to fundamental parameters of the Standard Model (SM), such as the  $|V_{cb}|$  and  $|V_{ub}|$  elements of the CKM matrix. Moreover, they can be used to test Lepton Flavour Universality (LFU), which states that the charged and neutral weak currents couple with the same strength to the three lepton families. In the SM, this is broken only by the Yukawa interaction that give different masses to the three families. The violation of LFU would be a clear indication of New Physics (NP) processes beyond the SM. It could manifest in differences in the decays of heavy-flavoured hadrons involving electrons, muons, taus (and their corresponding neutrinos), that go beyond the effects due to the different masses of the three charged leptons.

Recently, some intriguing anomalies have emerged in heavy-quark flavour physics that challenge the SM assumption of LFU and might allow to access a new level of fundamental interactions with far reaching implications. In particular, all measurements performed so far of the ratio of branching fractions for B-meson decays in final states with a  $(\tau, \nu_\tau)$  and a lighter  $(\ell, \nu_\ell)$  lepton pair  $\mathcal{R}(D^{*-}) \equiv \mathcal{B}(B^0 \rightarrow D^{*-} \tau^+ \nu_\tau) / \mathcal{B}(B^0 \rightarrow D^{*-} \ell^+ \nu_\ell)$ , where  $\ell = e$  or  $\mu$ , give results [1, 2, 3, 4, 5, 6] that are consistently higher than the SM prediction. The resulting world average [7] deviates from the SM prediction at four standard deviations, one of the largest anomalies in flavour physics. Theory interpretations of this discrepancy are prolific, with models containing additional charged Higgs bosons [8] or lepto-quarks [9, 10] being the most promising NP candidates.

Measurements of semileptonic decays at a hadron collider such as the LHC are challenging, due to the unknown momentum of the colliding partons and to the significantly worse environment with respect to B Factories in terms of particle densities, detector occupancy, trigger and detection efficiencies. However, due to the significant Lorentz boost and to the excellent performance of the LHCb vertex locator, the decay vertex of the  $b$  hadrons produced at the LHC is well separated from the primary interaction vertex. This gives the direction of the  $b$ -hadron momentum and enables to close the decay kinematics even in the presence of missing neutrinos. Indeed, LHCb performed measurements that were deemed to be unfeasible at hadron colliders, such as the first determinations at hadron colliders of  $|V_{ub}|$  using  $\Lambda_b \rightarrow p \mu \nu_\mu$  decays [11], and of  $\mathcal{R}(D^{*-})$  using the  $\tau^+ \rightarrow \mu^+ \nu_\mu \bar{\nu}_\tau$  decay [12]. In the following, a new LHCb measurement [13] of  $\mathcal{R}(D^{*-})$  by using the three-prong  $\tau^+ \rightarrow \pi^+ \pi^- \pi^+(\pi^0) \bar{\nu}_\tau$  decay is reported.

## 2. Measurement of $\mathcal{R}(D^{*-})$ by using three-prong $\tau$ decays

Three-prong  $\tau$  decays offer several advantages over leptonic decays. Firstly, due to the excellent performance of the LHCb vertex locator, the  $\tau$  decay vertex can be separated from the  $B$  decay vertex; this gives a powerful criterion to discriminate signal and the most abundant background source due to hadronic  $B$  decays with a  $D^{*-}$  and three pions in the final state. Secondly, the production of a single neutrino in each of the  $\tau$  and  $B$  decays, and the knowledge of the  $\tau$  and  $B$  directions, measured from their production and decay vertices, enable to close the decay kinematics and access the variables in the  $B$  rest frame with good resolution, thereby enabling the determination of the signal yield for branching fraction measurements. Thirdly, no charged leptons are present in the final state; this avoids the difficult task of discriminating  $B^0 \rightarrow D^{*-} \tau^+ (\rightarrow \ell \bar{\nu}_\tau \nu_\ell) \nu_\tau$  signal decays from the much more abundant background due to decays into lighter leptons, that might originate

not only from  $b$ -hadron decays, but also from semileptonic decays of charm hadrons further down in the decay chain, *i.e.*  $H_b \rightarrow D^{*-} H_c (\rightarrow X \ell \nu_\ell)$ .

In order to reduce experimental systematic uncertainties, the  $B^0 \rightarrow D^{*-} \pi^+ \pi^- \pi^+$  decay is chosen as a normalization channel. This leads to a measurement of the ratio

$$\mathcal{R}(D^{*-}) \equiv \frac{\mathcal{B}(B^0 \rightarrow D^{*-} \tau^+ \nu_\tau)}{\mathcal{B}(B^0 \rightarrow D^{*-} 3\pi)} = \frac{N_{\text{sig}}}{N_{\text{norm}}} \frac{\epsilon_{\text{norm}}}{\epsilon_{\text{sig}}} \frac{1}{\mathcal{B}(\tau^+ \rightarrow 3\pi(\pi^0) \bar{\nu}_\tau)}, \quad (2.1)$$

where  $3\pi \equiv \pi^+ \pi^- \pi^+$ , and  $N_{\text{sig}}$  ( $N_{\text{norm}}$ ) and  $\epsilon_{\text{sig}}$  ( $\epsilon_{\text{norm}}$ ) are the yield and selection efficiency for the signal (normalization) channel, respectively. From this,  $\mathcal{R}(D^{*-})$  is obtained as  $\mathcal{R}(D^{*-}) = \mathcal{H}(D^{*-}) \times \mathcal{B}(B^0 \rightarrow D^{*-} 3\pi) / \mathcal{B}(B^0 \rightarrow D^{*-} \mu^+ \nu_\mu)$ , where the branching fractions of the  $B^0 \rightarrow D^{*-} 3\pi$  and  $B^0 \rightarrow D^{*-} \mu^+ \nu_\mu$  decays are taken from Refs. [14] and [7].

After an initial preselection, the effective branching fraction of the main background process, due to  $b$ -hadron decays in final states containing a  $D^{*-}$  meson and three charged pions is two orders of magnitude larger than that expected for signal. However, due to the boost of  $b$  hadrons at the LHC and the detectable flight length of the  $\tau$  lepton at LHCb, the signal process results in a characteristic detached vertex topology (Fig. 1, left), where the  $\tau$  decay vertex lies downstream of the  $B^0$  decay vertex. This topology cannot occur in hadronic  $B \rightarrow D^{*-} 3\pi(X)$  decays. This background can therefore be rejected by three orders of magnitude, as shown in Fig. 1, right, by requiring that the difference of the positions of the  $3\pi$  and the  $B^0$  vertices along the beam direction, divided by its uncertainty, is greater than four. This requirement has an efficiency of 35% on signal. The normalization sample is selected by requiring the difference in the positions of the  $\bar{D}^0$  and  $3\pi$  vertices along the beam direction, divided by its uncertainty, to be greater than four.

The residual background, remaining after the detached vertex requirement, is due to  $B$  decays such as  $H_b \rightarrow D^{*-} (D_s^+, D^+, D^0) X$  where, due to its non-negligible lifetime, the second charm meson subsequently gives a detached  $3\pi$  system. The effective branching ratios for such decays are one order of magnitude larger than signal for  $H_b \rightarrow D^{*-} D_s^+ X$ , comparable to or smaller than

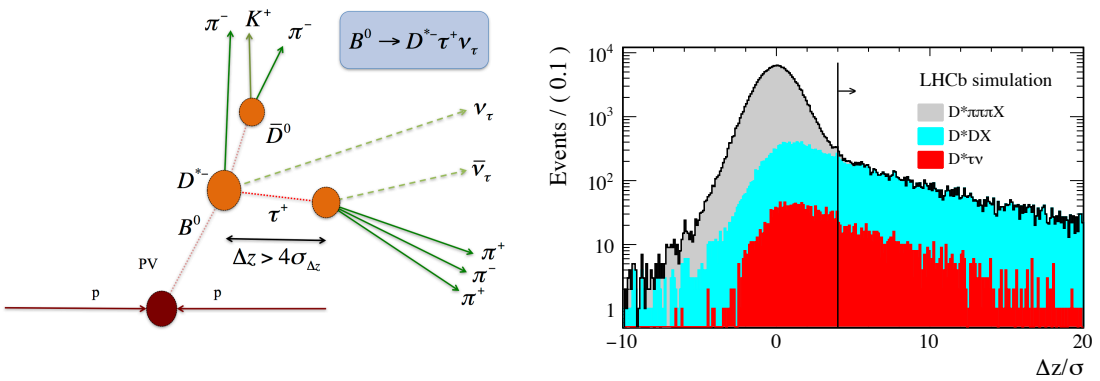


**Figure 1:** (left) sketch of the signal decay topology. (right) distribution of the distance between the  $B^0$  and  $\tau$  decay vertices, divided by its uncertainty. Signal is shown in red, background due to  $H_b \rightarrow D^{*-} \pi^+ \pi^- \pi^+ X$  in grey, background due to  $H_b \rightarrow D^{*-} H_c (\rightarrow \pi^+ \pi^- \pi^+ X') X$  decays in cyan, where  $H_b$  and  $H_c$  denote generic  $b$ - and  $c$ -hadrons,  $X$  and  $X'$  any unreconstructed particles.

signal for the other decays. This *double-charm background* is suppressed by applying vetoes on the presence of additional charged particles and neutral particle energy around the direction of the  $\tau$  and  $B$  candidates. The different resonant structure of the  $3\pi$  system in  $\tau$  and  $c$ -hadron decays is also exploited. A multi-variate analysis approach is used, where a Boosted Decision Tree (BDT) is trained to discriminate between signal and double-charm background.

Two neutrinos are emitted in the signal decay chain, giving six unknown quantities. The knowledge of the masses and lines of flight of the  $\tau$  and  $B^0$  give six constraints. The full decay kinematics can be therefore determined up to two-fold kinematic ambiguities. These can be resolved by choosing the maximum opening angles between the  $(\tau, 3\pi)$  and  $(B^0, D^{*-}\tau)$  systems. By using this approach, rest-frame variables such as the  $\tau$  decay time,  $t_\tau$ , and squared invariant mass of the  $(\tau, \nu_\tau)$  system,  $q^2$ , are reconstructed with negligible bias and an average resolution of  $1.17 \text{ GeV}^2/c^4$ , sufficient enough to preserve good discrimination between signal and background.

The signal yield is determined by performing a three-dimensional fit to data of the distributions of  $t_\tau$ ,  $q^2$  and BDT output. The fit components are described by templates obtained from simulation and corrected from control samples. In particular, the poorly-known contributions due to different  $H_b \rightarrow D^{*-}D_s^+X$  decays and their template shapes are determined from a fit of the  $D^{*-}D_s^+$  invariant mass in a sample where the exclusive  $D_s^+ \rightarrow 3\pi$  decay is reconstructed (Fig. 2, left). Also, the decays of the  $D_s^+$  meson in three charged pions and neutral particles are not well measured; the branching fraction of the exclusive  $D_s^+ \rightarrow 3\pi$  decay is only 1/15 of that of the inclusive  $D_s^+ \rightarrow 3\pi X$  decay. The relative contributions of such decays are determined by using a data control sample in a region of the BDT output that is rich in such decays (Fig. 2, right).

The fit projections on  $t_\tau$  and  $q^2$  for different BDT bins are shown in Fig. 3. A signal yield of  $1273 \pm 85$  candidates is determined, after a -3% correction due to a fit bias is applied. This bias is due to the presence of empty bins in the templates. A value of  $\mathcal{B}(D^{*-}) = (1.93 \pm 0.13_{\text{stat}} \pm$

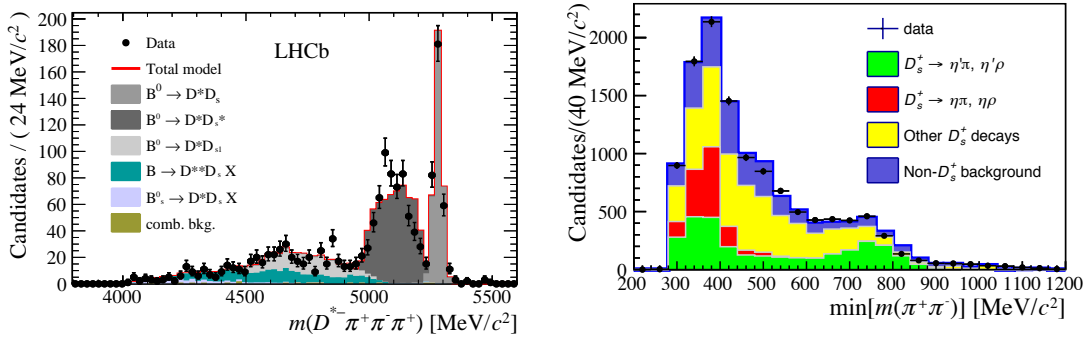


**Figure 2:** (left) Results from the fit to the  $D^{*-}D_s^+$  invariant mass for candidates in data containing a  $D^{*-}D_s^+$  pair, where  $D_s^+ \rightarrow 3\pi$ . The  $B^0 \rightarrow D^{*-}D_s^+$ ,  $B^0 \rightarrow D^{*-}D_s^{*+}$ ,  $B^0 \rightarrow D^{*-}D_{s0}^{*+}(2317)^+$ ,  $B^0 \rightarrow D^{*-}D_{s1}(2460)^+$ ,  $B^{0,+} \rightarrow D^{**}D_s^+X$  and  $B_s^0 \rightarrow D^{*-}D_s^+X$  components are shown as well. (right) Distributions of  $\min[m(\pi^+\pi^-)]$ , the minimum invariant mass of opposite-sign pions in the  $3\pi$  system, for a sample enriched in  $B \rightarrow D^{*-}D_s^+(X)$  decays, obtained by requiring the BDT output below a threshold. The different fit components correspond to  $D_s^+$  decays with (red)  $\eta$  or (green)  $\eta'$  in the final state, (yellow) all the other considered  $D_s^+$  decays, and (blue) backgrounds originating from decays not involving the  $D_s^+$  meson.

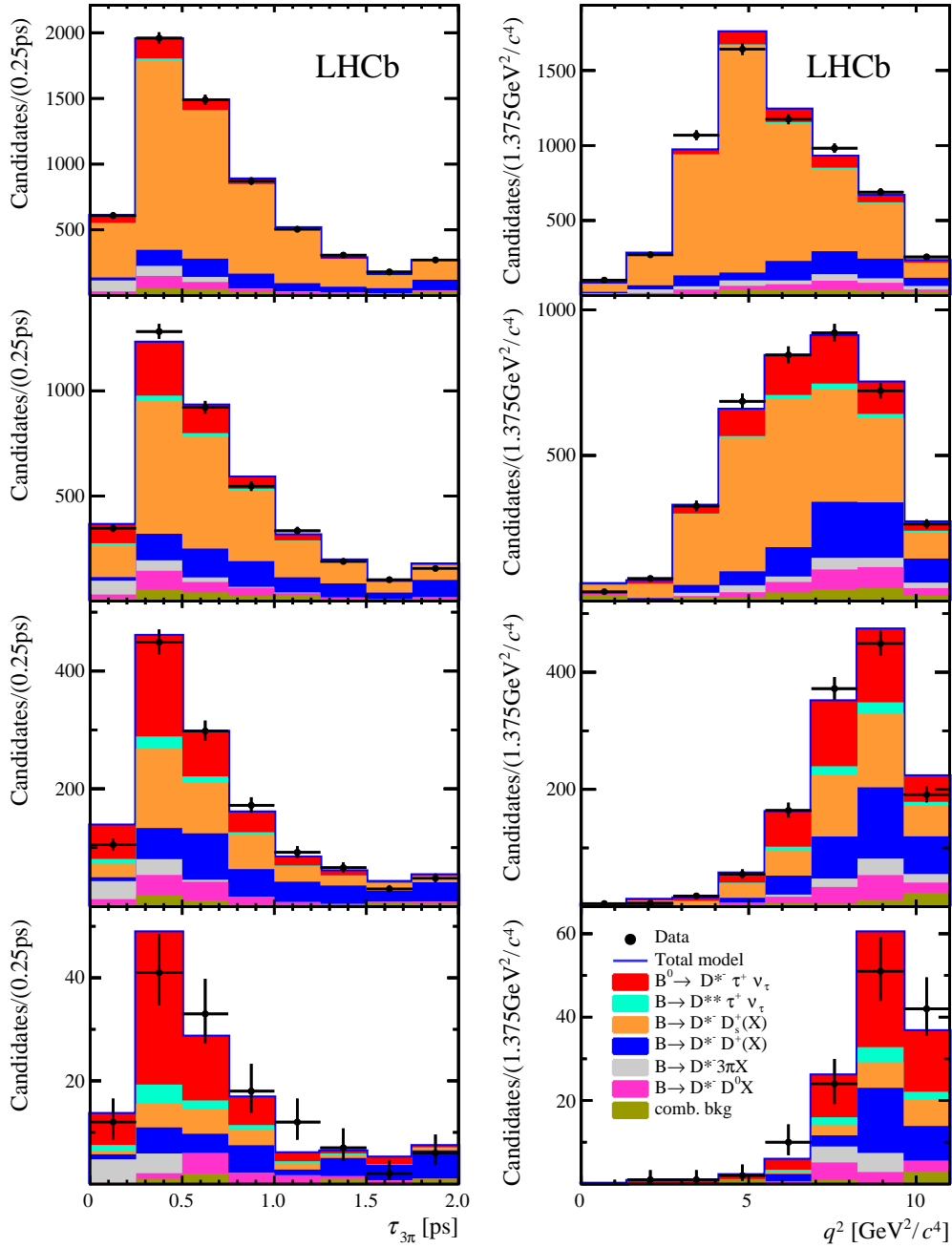


**Figure 3:** Fit projections on the (left)  $3\pi$  decay time and (right)  $q^2$  distributions for different BDT bins. The highest BDT bin corresponds to the two lower figures.

$0.17_{\text{sys}}$ ) is obtained, where the yield of the normalization modes (17, 000 candidates) is obtained by fitting the distribution of the  $D^{*-}3\pi$  invariant mass on candidates passing the corresponding selection criteria.

The dominant sources of systematic uncertainties are due to the size of the simulated sample (4.7%), to the knowledge of double-charm backgrounds and of the efficiency ratio between signal and normalization modes (3.9% each). The total systematic uncertainty is 8.9%. All the dominant uncertainties can be reduced in further updates of this analysis.

Using  $\mathcal{B}(B^0 \rightarrow D^{*-}3\pi) = (7.21 \pm 0.29) \times 10^{-3}$  from Ref. [14], a measurement of the absolute branching fraction of the  $B^0 \rightarrow D^{*-}\tau^+\nu_\tau$  decay is determined to be  $\mathcal{B}(B^0 \rightarrow D^{*-}\tau^+\nu_\tau) = (1.39 \pm 0.09_{\text{stat}} \pm 0.13_{\text{sys}} \pm 0.06_{\text{ext}}) \times 10^{-2}$ , where the third uncertainty originates from the knowledge of the branching fraction of the  $B^0 \rightarrow D^{*-}3\pi$  decay. The precision of this measurement is comparable to that of the current world average given in Ref. [14]. The first determination of  $\mathcal{R}(D^*)$  performed by using three-prong  $\tau$  decays is obtained by using the measured branching fraction of  $\mathcal{B}(B^0 \rightarrow D^{*-}\mu^+\nu_\mu) = (4.88 \pm 0.10) \times 10^{-2}$  from Ref. [7]. The result,  $\mathcal{R}(D^*) = 0.285 \pm 0.019_{\text{stat}} \pm 0.025_{\text{sys}} \pm 0.013_{\text{ext}}$ , represents one of the most precise measurements performed to date. It is one standard deviation higher than the SM prediction from Ref. [16], and consistent with previous measurements. An average of this measurement with the LHCb result using  $\tau^+ \rightarrow \mu^+\nu_\mu\bar{\nu}_\tau$  decays [12], accounting for small correlations due to form factors,  $\tau$  polarization and  $B \rightarrow D^{**}\tau^+\nu_\tau$  feeddown, yields a value of  $\mathcal{R}(D^{*-}) = 0.306 \pm 0.016_{\text{stat}} \pm 0.022_{\text{sys}}$ , consistent with the world average and 2.1 standard deviations above the SM prediction. The resulting combination in the  $\mathcal{R}(D), \mathcal{R}(D^*)$  plane (Fig. 4) is 4.1 standard deviations higher than the SM prediction. The new LHCb result slightly pulls down the value of the world average, but also slightly increases the SM discrepancy.

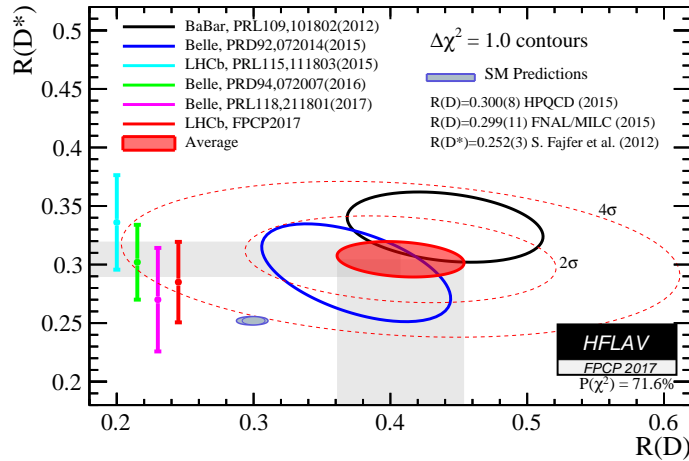


**Figure 4:** Current status of  $\mathcal{R}(D), \mathcal{R}(D^*)$  determinations, their average and comparison with SM predictions. Taken from [7].

### 3. Conclusion and outlook

LHCb is currently leading the studies of LFU through semi-tauonic decays of  $B$  mesons. A new measurement of the ratio  $\mathcal{R}(D^{*-}) = \frac{\mathcal{B}(B^0 \rightarrow D^{*-} \tau^+ \nu_\tau)}{\mathcal{B}(B^0 \rightarrow D^{*-} 3\pi)}$  using the  $\tau^+ \rightarrow \pi^+ \pi^- \pi^+ (\pi^0) \bar{\nu}_\tau$  decay leads to a first measurement of  $\mathcal{R}(D^*)$  with this final state, that is also one of the best single measurements of this quantity, having the smallest statistical error. The value  $\mathcal{R}(D^*) = (0.285 \pm 0.019_{\text{stat}} \pm 0.025_{\text{syst}} \pm 0.014_{\text{ext}})$  is compatible both with the SM prediction and with the world average. It slightly increases the discrepancy of the world average with respect to the SM from 4.0 to 4.1 standard deviations. This analysis was made possible due to the unique LHCb capabilities for separating secondary and tertiary decay vertices with excellent resolution. The method developed to perform this measurement paves the way for a whole program in the semitauonic decays of  $b$  hadrons. The  $\mathcal{R}(D^*)$  update using the full Run2 data is expected to reach 3% statistical precision and a significant reduction of systematic uncertainties. All other  $\mathcal{R}(X_c)$ , with  $X_c = D^0, D^-, D_s^-, \Lambda_c, J/\psi$ , can be determined, with measurements  $\mathcal{R}(\Lambda_c)$  and  $\mathcal{R}(J/\psi)$  currently underway. Finally, due to the unique possibility to isolate a high statistics, high purity sample of semitauonic decays, it is possible to study other variables in addition to the branching fractions, whose distributions can discriminate between the SM and various classes of NP models.

### References

- [1] J.P. Lees *et al.* (Babar Coll.), Phys. Rev. Lett. 109 (2012) 101802
- [2] J.P. Lees *et al.* (Babar Coll.), Phys. Rev. D88 (2013) 072012
- [3] R. Aaij *et al.* (LHCb Coll.), Phys. Rev. Lett. 115 (2015) 111803
- [4] M. Huschle *et al.* (Belle Coll.), Phys. Rev. D92 (2015) 072014
- [5] Y. Sato *et al.* (Belle Coll.), Phys. Rev. D94 (2016) 072007
- [6] S. Hirose *et al.* (Belle Coll.), Phys. Rev. Lett. 118 (2017) 211801
- [7] Y. Amhis *et al.*, arXiv:1612.07233 [hep-ex], accepted for publication in Eur. Phys. J. C, and further updates at <http://www.slac.stanford.edu/xorg/hflav/>.
- [8] M. Tanaka, Z. Phys. C67 (1995) 321
- [9] W. Buchmüller, R. Rückl and D. Wyler, Phys. Lett. B191 (1987) 442; erratum-ibid. B448 (1999) 320
- [10] S. Davidson, D.C. Bailey and B. Campbell, Z. Phys. C61 (1994) 613
- [11] R. Aaij *et al.* (LHCb Coll.), Nature Phys. 11 (2015) 743
- [12] R. Aaij *et al.* (LHCb Coll.), Phys. Rev. Lett. 115 (2015) 111803
- [13] R. Aaij *et al.* (LHCb Coll.), arXiv:1708.08856 [hep-ex]
- [14] C. Patrignani *et al.* (Particle Data Group), Chin. Phys. C40 (2016) 100001 and 2017 update.
- [15] J.P. Lees *et al.* (Babar Coll.), Phys. Rev. D94 (2016) 091101
- [16] S. Fajfer, J. F. Kamenik and I. Nisandzic, Phys. Rev. D 85 (2012) 094025